

Adsorption Ice making and Water Desalination System Using Metal Organic Frameworks/Water pair

Dakkama, Hassan; Youssef, Peter George; Al-Dadah, Raya; Mahmoud, Saad

DOI:

[10.1016/j.enconman.2017.03.036](https://doi.org/10.1016/j.enconman.2017.03.036)

License:

Creative Commons: Attribution-NonCommercial-NoDerivs (CC BY-NC-ND)

Document Version

Peer reviewed version

Citation for published version (Harvard):

Dakkama, H, Youssef, PG, Al-Dadah, R & Mahmoud, S 2017, 'Adsorption Ice making and Water Desalination System Using Metal Organic Frameworks/Water pair', *Energy Conversion and Management*, vol. 142, pp. 53-61. <https://doi.org/10.1016/j.enconman.2017.03.036>

[Link to publication on Research at Birmingham portal](#)

Publisher Rights Statement:

First checked 13/3/2017

General rights

Unless a licence is specified above, all rights (including copyright and moral rights) in this document are retained by the authors and/or the copyright holders. The express permission of the copyright holder must be obtained for any use of this material other than for purposes permitted by law.

- Users may freely distribute the URL that is used to identify this publication.
- Users may download and/or print one copy of the publication from the University of Birmingham research portal for the purpose of private study or non-commercial research.
- User may use extracts from the document in line with the concept of 'fair dealing' under the Copyright, Designs and Patents Act 1988 (?)
- Users may not further distribute the material nor use it for the purposes of commercial gain.

Where a licence is displayed above, please note the terms and conditions of the licence govern your use of this document.

When citing, please reference the published version.

Take down policy

While the University of Birmingham exercises care and attention in making items available there are rare occasions when an item has been uploaded in error or has been deemed to be commercially or otherwise sensitive.

If you believe that this is the case for this document, please contact UBIRA@lists.bham.ac.uk providing details and we will remove access to the work immediately and investigate.

Nomenclature

AC	Activated carbon, [-]	SrCl ₂	Strontium chloride
CaCl ₂	Calcium chloride [-]	T	Temperature, [K]
C _p	Specific heat, [kJ/kg/K]	t	Time, [sec]
COP	Coefficient of Performance, [-]	Subscript	
CO ₂	Carbon dioxide [-]	ads	Adsorption
<i>m</i>	mass	AF	Anti-freeze
\dot{m}	Mass flow rate [kg/sec]	at	Adsorption time
Q_{evap}	Refrigeration effect, [kW]	ct	Cycle time
Q_{heat}	Consumed heat power, [kW]	des	desorption
MOF	Metal Organic Framework [-]	evap	Evaporator
N	Number [-]	hct	Half cycle time
RTD	resistance temperature detectors	in	inlet
SDIP	Specific Daily Ice Production [ton/day/ton_ads]	out	outlet
SDSP	Specific Daily Ice Slurry Production [ton/day/ton_ads]	w	water
SDWP	Specific Daily Water Production [ton/day/ton_ads]		

29

30 **1. Introduction**

31 There is a growing demand for fresh water and cooling in many developing countries where access to electricity
32 is limited [1]. The International Institution of Refrigeration (IIR) has reported that about 15% of the entire
33 electrical power generation in the world is consumed for refrigeration and air conditioning applications.
34 Furthermore, the World Health Organization (WHO) has reported that 884 million people have no access to fresh
35 water and more than 2.4 billion have a limited access [2].

36 There are many applications for ice like preservation of medical products (vaccine), frozen food (fish, meat,
37 vegetables), chemical engineering processes, thermal energy storage and freeze desalination [3]. The use of
38 conventional vapor compression system cooling system for ice making consumes significant amount of
39 electricity leading to high Carbon dioxide (CO₂) emissions. In order to reduce the demand of electricity, the heat
40 driven cooling systems like adsorption and absorption systems are alternative cooling systems [4]. Absorption
41 system has the advantage of higher Coefficient of Performance (COP) compared to the adsorption system [5].
42 However, there are many disadvantages like contamination, crystallization and corrosion [6]. Therefore,
43 adsorption cooling technology can be used due to its advantages of stability and the use of environmentally
44 friendly working pairs [7].

45 Adsorption ice making systems were experimentally and theoretically investigated by researchers using various
 46 working pairs as shown in Table (1). The majority of researchers used activated carbon as adsorbent with
 47 methanol and ammonia as refrigerants. This is due to the potential of such working pairs to achieve the cooling
 48 effect for ice making application, as the freezing point of refrigerants are lower than that of water.

49

50 **Table 1** List of adsorption ice making systems

Ref.	Working pair	$m_{\text{adsorbent}} / m_{\text{refrigerant}}$ [kg/kg]	SDIP [ton/day/ton_ads]	COP [-]	T_{evap} [°C]	T_{des} [°C]	Heat source
[5]	(CaCl ₂ /AC)/Ammonia	30/_	1.66	0.15	-5	105	solar
[8]	AC/ methanol	44 / 3.23	0.16-0.227	0.452	-1	90-100	solar
[9]	AC NORIT RX3-Extra/ methanol	14/4.3	0.357-0.93	0.42	-4	108	solar
[10]	AC / methanol	20/_	0.35-0.5	0.24	-0.9	115	solar
[11]	AC / methanol	17/_	0.235-0.3	0.12	-6	78	solar
[12]	AC / methanol	22/3.3	0.46	0.38	-2.5	98	solar
[13]	AC /methanol	112/_	0.118	0.086	-11	110	Waste heat
[14]	AC/ Methanol	130/20	0.23-0.26	0.43	-3	N/A	solar
[15]	AC (MD6070)-methanol	N/A	0.6417-0.747	0.6	-3	N/A	solar
[16]	AC/ Methanol	20/_	0.26-0.35	0.12		N/A	solar
[17]	lithium chloride in silica gel pores- methanol	36/_	0.83	0.33	-6	N/A	N/A
[18]	AC–Ammonia	16.99/1.38	0.235	0.25	0	N/A	solar
[19]	SrCl ₂ – ammonia	22/15	0.527	0.069	-15	93	solar
[20]	AC/ Methanol	19/0.4	0.37-0.473	0.15			
[21]	AC / methanol	20/_	0.2-0.3	0.11	-0.5	N/A	solar
[22]	AC/methanol	29/	0.224	0.122	-2	93	solar
[23]	Zeolite / water	16 / 4	0.3125	0.08	0	180	solar
[24]	Zeolite/Water	75.5 / _	0.09	0.8	-2.8	_	solar
[25]	AC-CaCl ₂ / water	N/A	N/A	0.39	-20	114	N/A
[26]	Zeolite /water	4.2/_	N/A	0.25	N/A	200-300	N/A

51

52

53

54 The table shows that the values of specific daily ice production (SDIP) ranged from 0.03 to 1.66 ton/day/ton_ads
55 (or kg/day/kg_ads). The maximum value (1.66 ton/day/ton_ads) was experimentally achieved using compound
56 adsorbent Calcium chloride/Active Carbon (CaCl_2/AC) /Ammonia as a working pair with COP of 0.15 using a
57 parabolic trough solar collector to supply the heat energy for the adsorption ice making system [5]. Up to now,
58 only few studies, as shown in the Table 1, have used the zeolite-water as working pair for ice making
59 applications using high generation temperature up to 180°C to achieve SDIP ranging from 0.09 to 0.3125
60 ton/day/ton_ads and COP ranging from 0.08 to 0.8. There are many advantages of water to be used as
61 refrigerant like, environment friendly, high latent heat of evaporation and low cost. At vacuum operating
62 pressure, water boils at low temperature reaching freezing point of water about zero $^\circ\text{C}$ leading to formation of
63 ice. However, the water is commonly recommended to use as refrigerant in air conditioning applications [27].
64 Many of researchers stated that water cannot be used for freezing application due to the restriction of its freezing
65 point [26]. Adsorbent material is one of the main factors that affect the performance of adsorption ice making
66 system [28]. Many solid sorbents like activated carbon (AC), Chloride strontium (SrCl_2), zeolite, Metal hydride
67 (MnCl_2), consolidated composite AC, binary salt $\text{BaCl}_2+\text{BaBr}_2$, lithium chloride and compound adsorbent
68 (CaCl_2/AC) have been used in the previously reported adsorption ice making systems (see table 1). The
69 advantage of the stated adsorbents is the high stability; however, there is a drawback in terms of low refrigerant
70 adsorption capabilities, thus affecting the performance of adsorption ice making system in terms of SDIP.
71 Metal Organic Frameworks (MOFs) are new type of solid sorbent materials, which have high pore volume, high
72 surface area, uniform pore size and robustly tunable structural properties. The MOF materials have been already
73 tested for gas storage, gas separation, sensors catalysis automotive air conditioning, water adsorption
74 applications [28]. Other applications including thermal energy storage, low temperature cooling and water
75 desalination were investigated using the MOF materials [29]. Some researchers have experimentally and
76 numerically investigated a nickel based coordination polymer with open metal sites of organic frameworks
77 (CPO-27(Ni)) with water to use for adsorption desalination application or thermal storage application. They
78 highlighted that CPO-27(Ni) has an advantages in terms of SDWP at low evaporation temperature up to 5°C
79 compared to other MOFs [30].

80 Ice slurry is used in many applications like refrigeration systems, food industry and freezing desalination at
81 different temperatures from -5 to -35°C with refrigerants used are either organic or non-organic refrigerants like
82 1,1-Dichloro-1-fluoroethane (R141b) [31]. Regarding the freeze desalination, many researchers used sea water
83 to produce a mixture of ice slurry and brine, then, this mixture is processed through separation and

84 filter/washing stage to remove any saline solution to obtain potable water [31]. A significant amount of energy
85 was consumed in the cooling and separating processes based on conventional method [32].
86 Current desalination techniques are: Reverse Osmosis (RO), multi stage flash distillation (MSF) and multi effect
87 distillation [30]. The RO is the most efficient technique in terms of energy consumption but suffer from
88 contamination of chloride, bromide and boron, high maintenance cost and limited validity of membrane life [2].
89 In addition, the only outcome of such technologies is fresh water and no cooling can be achieved [33].
90 Adsorption desalination system offers the potential of producing distilled water and cooling as two useful
91 outputs [34] using the same heat source. The sea water is the main refrigerant while silica gel and zeolite are the
92 commonly used adsorbents materials in the adsorption desalination system [34].
93 In the above literature, the adsorption technique was used for either ice making or desalination and cooling
94 purposes and there is no reported work that combines ice making with desalination and cooling. In addition,
95 there is no published work on using water or saline water as refrigerant in the production of ice, ice slurry or
96 freeze desalination applications. This paper experimentally investigates a new technique (vacuum-direct
97 freezing) of single bed adsorption system to produce four useful outputs; ice, cooling, ice slurry and distilled
98 water using both tap and sea water as refrigerants with CPO-27Ni Metal Organic Framework adsorbent
99 material. In order to find the optimum performance of the adsorption ice making-water desalination, four
100 parameters are investigated, namely, number of cycles, switching time, adsorption - desorption time and salinity
101 effect. The outputs of this system are evaluated in terms of specific daily production of solid ice (SDIP), slurry
102 (SDSP) and fresh water (SDWP), as well as the coefficient of performance based on cooling (COP).

103

104 **2. Vacuum Direct Freezing**

105 The main difference between this approach and the conventional adsorption cooling system is the production of
106 multi-outputs like ice, ice slurry (flake) and cooling effect compared to the production of only cooling in the
107 conventional system. This is achieved through using the seawater as the main refrigerant in the evaporator and
108 pure water cups for ice production in addition to the cooling coil. Therefore, when adsorption process occurs,
109 evaporation of the pure water in the cups will lead to freezing producing solid ice while the saline water will
110 crystallize producing ice slurry. At the same time, the chilled fluid passing through the coil receives cooling effect.
111 The crystallization phenomenon of solid ice occurs due to the vacuum operating conditions produced by
112 adsorption process during a certain period until the upper surface of fresh water will be frozen. The
113 crystallization phenomenon continues according to the heat transfer with the saline water through the wall's

114 cups. An external load was applied in the evaporator by circulating antifreeze through the evaporator's coil to be
115 cooled down. The coil was immersed in the refrigerant liquid where a heat transfer will be achieved and the
116 cooling effect of the antifreeze will be produced as a third output.

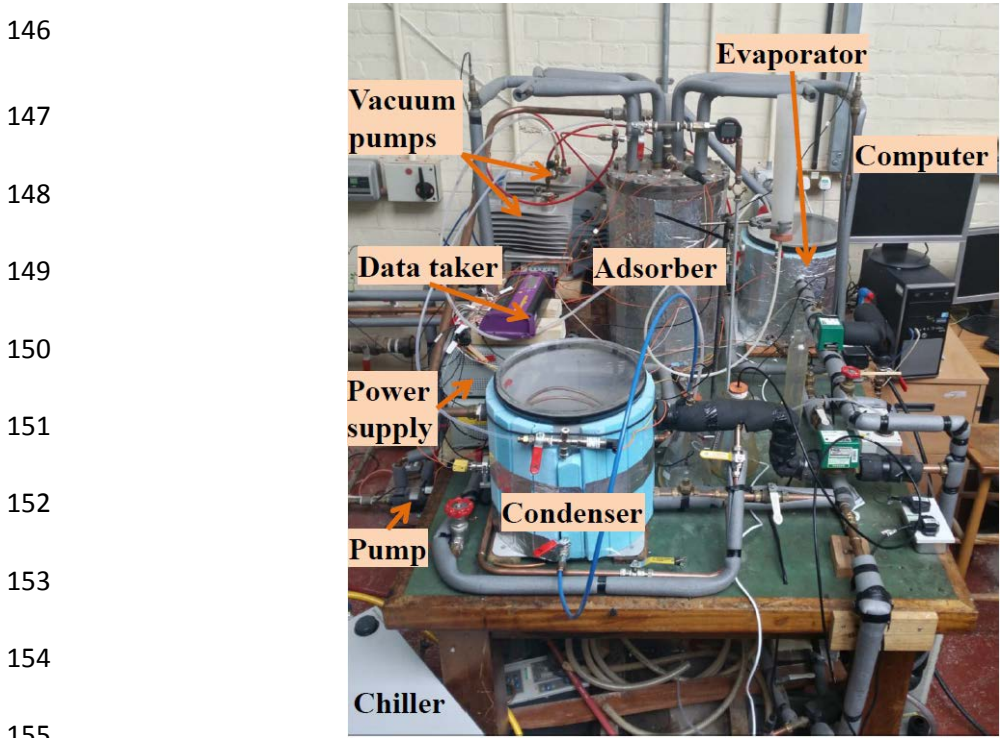
117

118 **3. Description of the Test Facility**

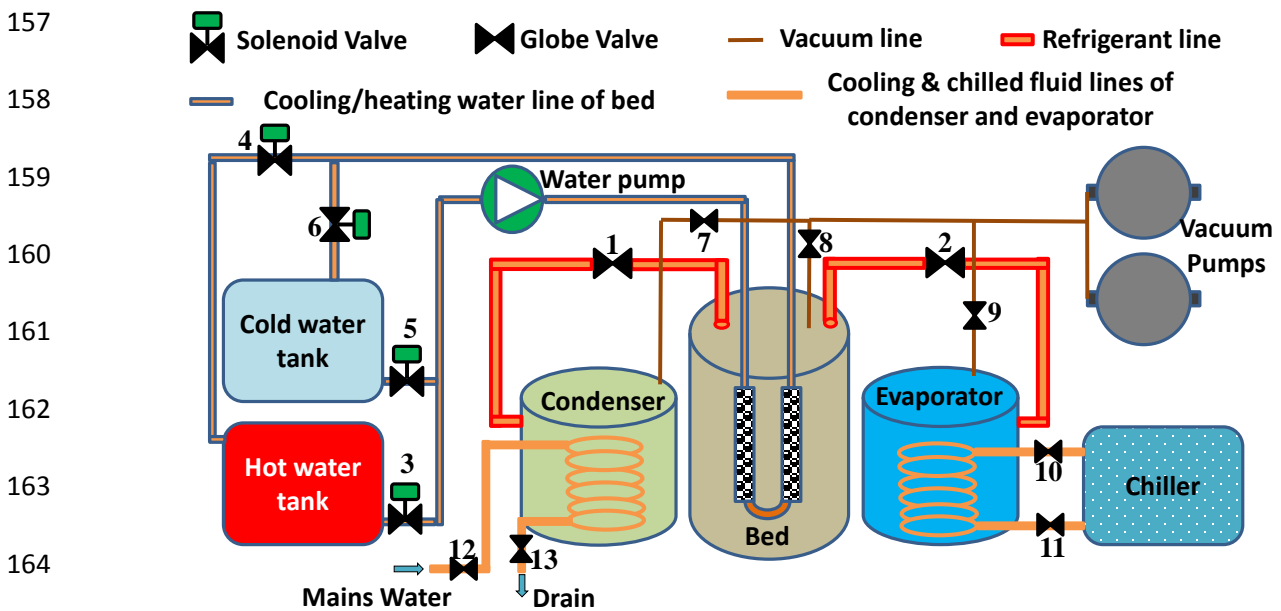
119 Fig. 1 and 2 show pictorial and schematic diagrams of the experimental test facility for the adsorption system
120 consisting of adsorber bed, condenser and evaporator. The adsorber bed consists of steel cylinder and pair of
121 finned tube heat exchangers in which 670 grams of CPO-27 (Ni) is packed in the spaces between the fins. Metal
122 mesh was used to cover the heat exchangers to keep the adsorbent material between the fins. The adsorber was
123 connected to heating and cooling systems (liquid side) through four solenoid valves to automatically control the
124 flow direction of water. Two shell and coil heat exchangers were made to work as the condenser and evaporator
125 for the system. The shells are provided with transparent lids to view the condensation and evaporation-freezing
126 processes in which the fresh water and ice, ice slurry could be collected from the condenser and evaporator,
127 respectively. The condenser is cooled using mains water, while the evaporator is heated by circulating chilled
128 antifreeze-water mixture with solenoid valves used to control flow direction of the main water and chilled
129 antifreeze-water mixture, respectively. The solenoid valves are controlled using a control board, which is
130 connected to a computer and controlled using LabView.

131 Many measuring instruments are fixed in the test facility for measuring the temperatures, flow rate and
132 pressures. Five thermocouples (type T) with an accuracy of $\pm 0.5^{\circ}\text{C}$ are fitted on the adsorber bed to measure the
133 adsorbent temperature at different positions. The inlet and outlet temperatures of hot/cold water flow to the
134 adsorber are measured using two resistance temperature detectors (RTDs) with an accuracy of $\pm 0.3^{\circ}\text{C}$. Another
135 pair of thermocouples (type T) is fitted in the evaporator to measure the vapor and liquid temperatures of
136 refrigerant, while the inlet and outlet temperatures of chilled antifreeze are measured using two RTDs. The
137 condenser is provided with two thermocouples (type K) to measure the refrigerant vapor and liquid
138 temperatures. The inlet and outlet temperatures of cooling water in the condenser were measured using two
139 RTDs. The inlet mass flow rate of heating/cooling water to the adsorber bed is measured using FLC-H14 flow
140 meter from Omega with the range of 0-57 LPM and accuracy of $\pm 1\text{LPM}$. The inlet mass flow rate of the chilled
141 antifreeze is measured using EFW.0302 flowmeter from Parker with range of 2-30 LPM and accuracy of $\pm 5\%$.
142 The pressure in the adsorber bed, condenser and evaporator are measured using three pressure transducers with
143 range of 0 to 350 mbar (absolute pressure) and an accuracy of $\pm 0.01\text{kPa}$ and current output signal ranging from

144 four to 20 mAmp. A data taker is used to log the output signals of measuring instruments every 4 seconds,
 145 which are monitored using personal computer.



156 **Fig. 1.** Pictorial view of adsorption ice making and water desalination system



168 **Fig. 2.** The schematic diagram of adsorption ice making and water desalination system

168 **4. Experimental Procedure**

169 The following steps explain the practical procedure in details, including preparing and operation.

170 **4.1 Preparing Procedures:**

171 There are many preliminary procedures, which are required to prepare the current system before each run to be
172 operated at same initial conditions (see Table 2) and obtained reliable results. Firstly, connect the adsorber bed
173 to the heating water system and a vacuum pump by opening valves 3, 4 and 8, as shown in table 3, to remove
174 any refrigerant from the adsorbent material. This task was finished when the pressure and temperature of adsorber
175 bed reaches to certain values of 7 mbar and 85°C, respectively. Secondly, connect the condenser to the vacuum
176 pump by opening valve 7 until the pressure and temperature in the condenser reaches to certain values of 2 mbar
177 and 23°C, respectively. Thirdly, dissolve a required mass of a real sea salt with two liters of deionized water to
178 obtain the required value of total dissolved solids of sea water (i.e. 35000 ppm based on 70grams of real sea
179 salt). Fourthly, pour the two liters of sea water (as refrigerant) in the evaporator's shell for the purpose of ice
180 slurry producing, and then immerse 16 of stainless steel cups (480 mL) [3] by filling them with fresh water for
181 the purpose of ice making. Finally, the vacuum pumps were connected to the evaporator by opening valve 9 for
182 a period of 5min, thus, pressure inside the evaporator reach to 6mbar based on the liquid temperature of
183 refrigerant of 1°C.

184 **Table 2** Operating and initial conditions for the parametric study of the test facility.

185

<i>Parameter</i>	<i>Value</i>	<i>Unit</i>
Ambient temperature	23	°C
Mass flow rate of heating/cooling water system	7.3	L/min
Mass flow rate of chilled anti-freeze	5	L/min
Mass flow rate of tap water in condenser	5	L/min
Specific heat of water	4.18	kJ/kg/K
Specific heat of anti-freeze	4.1	kJ/kg/K
Preparing time	8	min
Total adsorbent mass	670	gram
Average temperature of inlet tap water	15	°C
Average temperature of inlet chilled antifreeze	-1	°C
Average temperature of heating water	95	°C
Average temperature of cooling water	20	°C
Volume of sea water in evaporator	2	L

186

187 **4.2 Operation Procedures**

188 At the end of preparing procedures, the system is ready to be operated and four steps were required to run the
 189 system and obtain the results. Firstly, the evaporator and condenser were connected to the chiller and main water
 190 line by opening valves 10, 11, 12 and 13 to circulate the antifreeze and cooling water at certain temperatures,
 191 respectively. Secondly, the adsorber was connected with the cold water system (liquid side) by opening valves 5
 192 and 6 to achieve a pre-cooling process during a required switching time. Thirdly, the adsorber was connected to
 193 the evaporator (refrigerant side) by opening valve 2 to start the adsorption process during the half cycle time, by
 194 continuing the circulation of cooling water with the adsorber to shed a heat, which is generated during the
 195 adsorption process. At the end of this task, close the valves 5, 6 and 2 to isolate the generator from the
 196 evaporator and cooling water system. Fourthly, the adsorber was connected to the heating water system (liquid
 197 side) by opening valves 3 and 4 to prepare it for a next mode which is desorption phase at the same switching
 198 time. Fifthly, the adsorber was connected with the condenser (refrigerant side) by opening valve 1 to start a
 199 desorption-condensation process during the same half cycle time of adsorption process. Finally, the solid ice and
 200 ice slurry were collected from the evaporator to calculate the specific daily production of ice (SDIP) and slurry
 201 (SDSP), respectively. In addition, the fresh (distilled) water was collected from condenser to calculate the
 202 specific daily water production (SDWP) of the system.

203 **Table 3** Control sequence and valves operation for the test facility.

	Description	Time (min)	Valve 1	Valve 2	Valve 3	Valve 4	Valve 5	Valve 6	Valve 7	Valve 8	Valve 9	Valve 10	Valve 11	Valve 12	Valve 13
Preparing Period	Bed-vacuum pump	-	M	M	A	A	A	A	M	M	M	M	M	M	M
	Condenser-vacuum pump	-	M	M	A	A	A	A	M	M	M	M	M	M	M
	Evaporator-vacuum pump	-	M	M	A	A	A	A	M	M	M	M	M	M	M
Operation period	Switching time-precooling	3	M	M	A	A	A	A	M	M	M	M	M	M	M
	Adsorption-evaporation	16	M	M	A	A	A	A	M	M	M	M	M	M	M
	Switching time-preheating	3	M	M	A	A	A	A	M	M	M	M	M	M	M
	Desorption-condensation	16	M	M	A	A	A	A	M	M	M	M	M	M	M
A	Closed valve/Automated control (LabView)	M	Closed valve/ manually control												
A	Opened valve/Automated control (LabView)	M	Opened valve/ manually control												

212

213

214 **5. SYSTEM PERFORMANCE ANALYSIS**

215 The coefficient of performance (COP) of adsorption ice making and freeze desalination system was defined as
 216 the ratio of effective cooling capacity in the evaporator and the regeneration heat in adsorber The calculation was
 217 based on the temperatures of liquid and antifreeze side as given by,

$$218 \quad COP = \frac{Q_{evap}}{Q_{heat}} \quad (1)$$

219 In equation (1), Q_{evap} was the refrigeration effect during the adsorption time. Q_{heat} was the consumed heat for the
 220 preheating and desorption process. They were evaluated using equations (2) and (3) as follows,

$$221 \quad Q_{evap} = \frac{\dot{m}_{AF} C_{pAF}}{t_{at}} \int_0^{t_{at}} (T_{AF,in} - T_{AF,out}) dt \quad (2)$$

$$222 \quad Q_{heat} = \frac{\dot{m}_{w,hot} C_{p,w,hot}}{t_{hct}} \int_0^{t_{hct}} (T_{hot,w,in} - T_{hot,w,out}) dt \quad (3)$$

223 The Specific Daily Ice Production (SDIP) was calculated using equation (4) based on the collected mass of solid
 224 ice from the evaporator (fresh water in the cups). The required time between two batches was taken in to
 225 account as 8 min for collecting the ice and evacuating process in task (e) of preparing procedures as follows:

$$226 \quad SDIP = \frac{m_{ice,batch} \times 60 \times 24}{(t_{ct} \times N_{cycle/batch} + t_{preparing}) \times m_{ads}} \quad (4)$$

227 The Specific Daily Ice Slurry Production (SDSP) was calculated using equation (5) based on the collected mass
 228 of ice slurry from the evaporator (seawater side). The required time between two batches was also taken in to
 229 account as follows:

$$230 \quad SDSP = \frac{m_{ice_slurry,batch} \times 60 \times 24}{(t_{ct} \times N_{cycle/batch} + t_{preparing}) \times m_{ads}} \quad (5)$$

231 The Specific Daily Fresh Water Production (SDWP) was calculated based on the collected mass of fresh water
 232 from the condenser as given in equation (6). The required time between two batches was also taken in to
 233 account as follows:

$$SDWP = \frac{m_{water,batch} \times 60 \times 24}{(t_{ct} \times N_{cycle/batch} + t_{preparing}) \times m_{ads.}} \quad (6)$$

235

236 6. RESULTS

237 In this section, parametric studies of the test facility are experimentally analyzed and discussed based on four
 238 parameters by investigating the performance of the adsorption ice making-water desalination system and finding
 239 the optimum conditions. Regardless the studied parameters, the parametric studies were conducted at same initial
 240 and operating conditions (see Table 2). For each experiment of the parametric studies, the uncertainties were
 241 assessed based on the calibrations of the measurement instruments. The uncertainty in the SDIP, SDSP, SDWP
 242 were estimated based on the calibration of a scale and a beaker which were used to measure the outputs, while for
 243 the COP, it was assessed based on the calibration of the thermocouples and flow meter, as follows:

244

245 6.1 Salinity Effect of Sea Water

246 Fig. 3 (A), (B), (C) and (D) show the salinity effect of water as the refrigerant in evaporator on the performance
 247 of the adsorption ice making-water desalination system. As shown in Fig. 3(A), it is clear that the optimum
 248 SDIP was at 35 ppm based on maximum mass of the produced ice in cups per batch. There was a slight increase
 249 in the SDIP by 7.7% when the salinity was increased from 20 to 35 ppm. This is due to the potential of water to
 250 evaporate for longer time before starting frozen in the evaporator. Then the SDIP started to slightly drop to 1.3%
 251 per 15×10^3 ppm by increasing the salinity from 35 to 65 ppm. Fig. 3(B) shows that there were sharp increases in
 252 the SDSP and SDWP up to 60% and 6.3% by increasing the salinity from 20 to 35 ppm, respectively. The same
 253 trend was shown in Fig. 3 (C) but with slight effect on the COP. The reason for this is because the period of
 254 evaporation-adsorption processes is relatively increased by lowering the freezing point of water. In contrast, the
 255 SDSP, SDWP and COP are moderately decreased by increasing the salinity of water from 35 to 65 ppm. This is
 256 may be caused by changing the physical properties of water which leads to drop in SDSP, SDWP and COP.

257

258

259

260

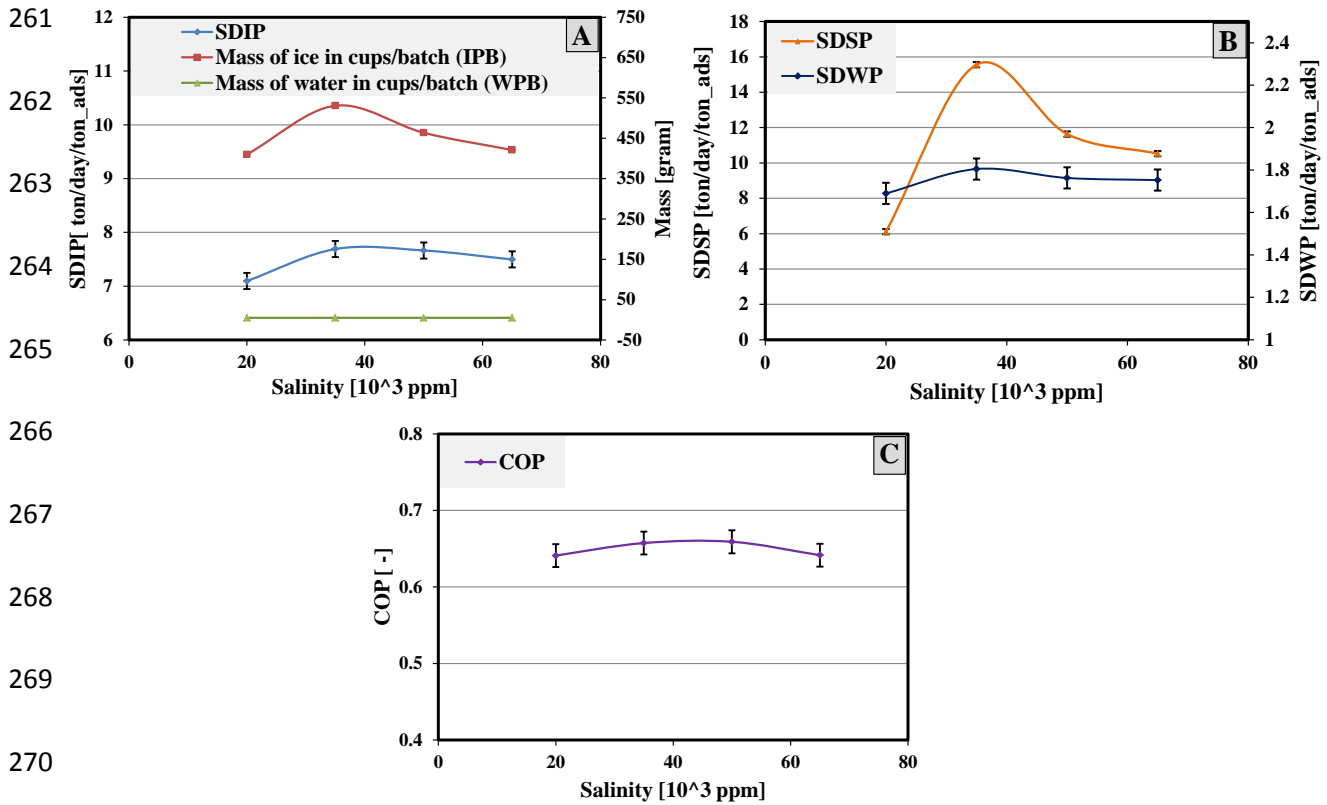


Fig. 3. Effect of water salinity on each of (A) SDIP, mass of solid ice and fresh water in the evaporator, (B) SDSP in the evaporator and SDWP in the condenser, and (C) COP of cooling.

6.2 Effect of cycle's number

Fig. 4 shows the effect of cycle's number on the performance of adsorption ice making – water desalination system in terms of the COP, SDIP, SDSP and SDWP. It can be seen in Fig. 4(A) that the overall trend of the SDIP shows fluctuation between 8.4 to 7.5 ton/day/ton_ads by increasing the cycle's numbers from 1 to 4. Despite this trend, the mass of solid ice in stainless steel cups per batch increased considerably by increasing the cycle's numbers. This is because the batch/run time, as by increasing the number of cycles, the batch time will be increased, in turn; the increase in mass of solid ice may not be noticed according to the operating time during the whole day period. For example the batch/run time of one and four cycles is up to 34 and 112 mins (including the preparing time) where the same number of the cups was used in the both tests, in which the ice formed at different run times. Fig. 1 shows that there was water in the stainless steel cups after 1st, 2nd and 3rd cycles while the all water in the cups is crystallized to solid ice at the 4th cycles. This is due to the improvement in ice production per batch, as the solidity of ice is directly proportional with the number of cycles according to the longer time of cooling effect based on the same amount of fresh water in the 16 cups.

286 Fig. 4(B) shows that the SDSP is significantly decreased by 30.4%, 15.3% and 12.8% per one cycle by
287 increasing the number of cycles from one to four cycles, respectively. In spite of this drop in SDSP the mass of
288 ice slurry is considerably increased by 30.9%, 26.6% and 11.8% per one batch by increasing the cycle's number
289 from 1 to 4, respectively. This is due to the day time, where the rate of increase in ice slurry per batch dose not
290 overcomes the increase in run time itself which has inversely effect on the SDSP during a period of whole day.
291 The increase in ice slurry mass per batch is due to the highly potential of sea water (as refrigerant) to freeze in
292 evaporator, according to the evaporation process will be increased which leads to increase the amount of ice
293 slurry per batch.

294 As shown in Fig. 4(C), the cycle's numbers effects on the cooling COP as it is clear to notice that the COP of
295 one and two cycles is up to 0.3, and based on this value, the COP drops down by about 60% and 73% with three
296 and four cycles, respectively. The reason of this drop belongs to the potential of the ice slurry to be formed on
297 the exposure surface in the evaporator is higher than the one and two cycles. Accordingly, the evaporation-
298 adsorption process between the evaporator and bed will be weaker than in case of one and two cycles.

299 Fig. 4(D) shows that there were an enhancement in the SDWP up to 78% and 24 % per one cycle by increasing
300 the cycle's number from one to three cycles, respectively. In the same figure, there was a drop in the SDWP
301 after the third cycle. However, despite this drop, the mass of distilled water in condenser is significantly
302 increased per one batch by increasing the number of cycles. The main cause of this drop is the day time as it will
303 be affected on the water production in condenser per day. The figure also shows that the one cycle per batch
304 produced small amount of water (4 grams) in condenser due to the adsorbent in the bed has low potential to
305 release the vapour to the condenser as some of refrigerant stuck in the adsorbent which needs longer time to
306 release the vapour to the condenser.

307

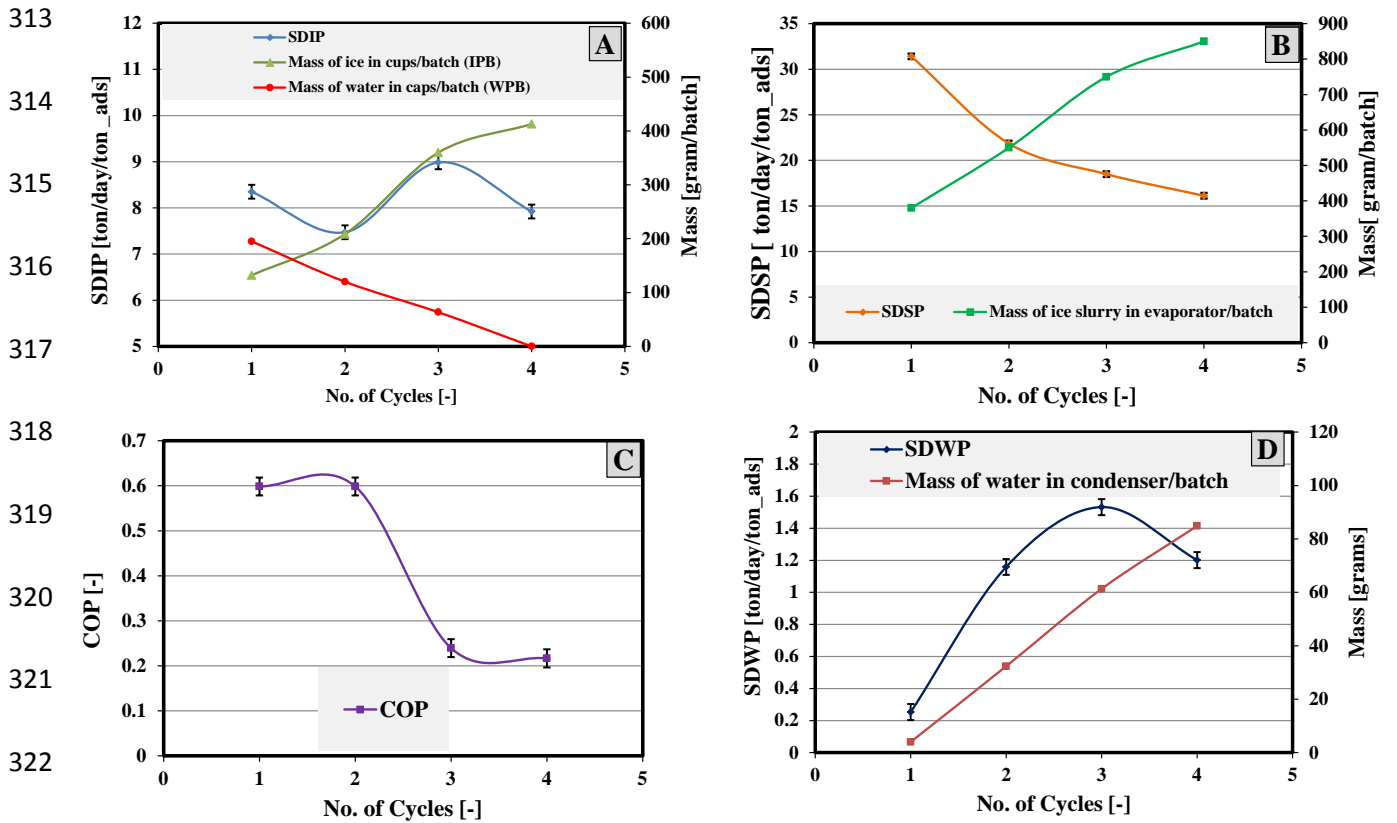
308

309

310

311

312



323 **Fig. 4.** Effect of cycles number on the each of (A) SDIP, mass of solid ice and fresh water in the evaporator,(B) SDSP
 324 and mass of ice slurry in the evaporator ,(C) SDWP and mass of fresh water in the condenser and (D) COP of cooling.

325 6.3 Effect of Switching Time

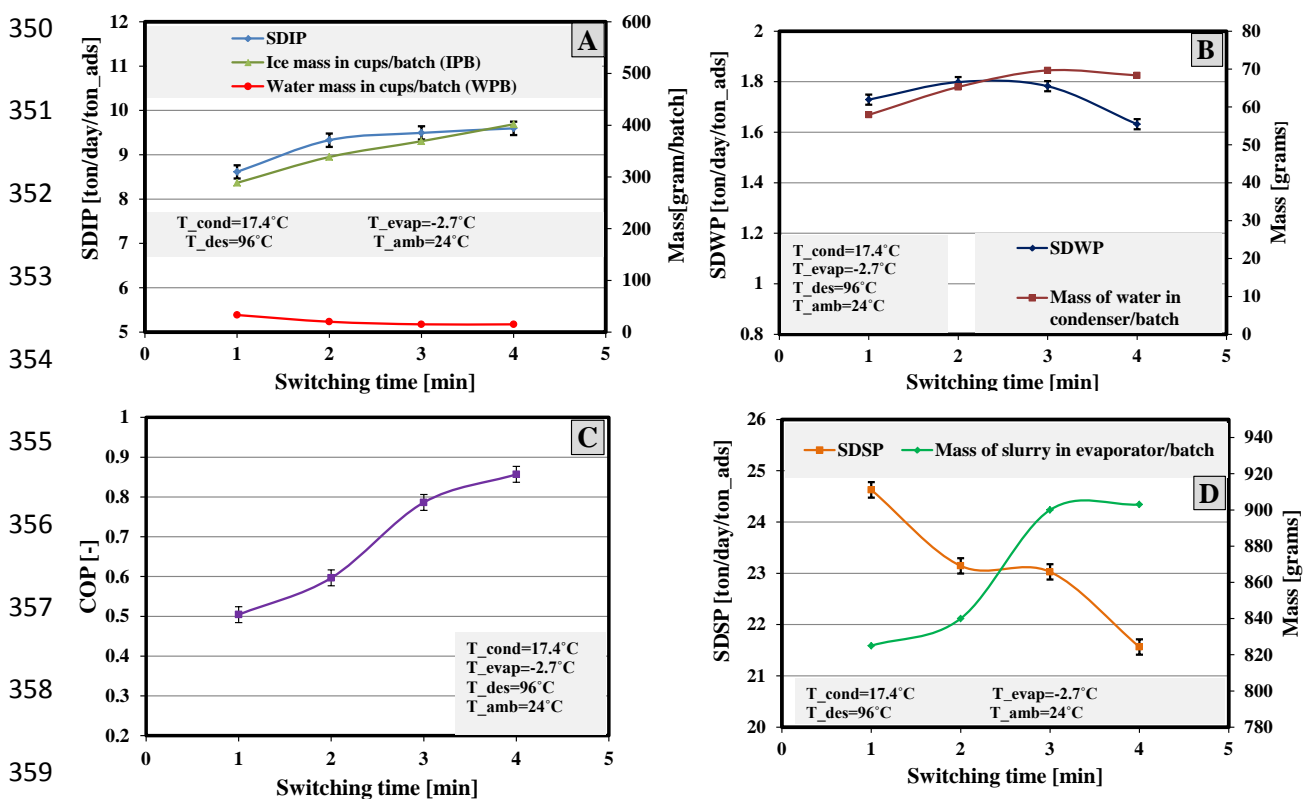
326 Fig. 5 shows that the impact of switching time on the SDIP, SDSP, SDWP, and COP based on the selected
 327 cycles number of 3 cycles per batch as shown in the previous section. As shown in Fig. 5(A), there were small
 328 enhancements on the SDIP up to 7.6% 1.7% and 1% per one min by increasing the switching time from one to
 329 four, respectively. This is because that the adsorbent (at high switching time) will take a longer time for pre-
 330 cooling and pre-heating, in turn, the bed will be prepared to absorb and release high amount of refrigerant
 331 vapour from evaporator and to condenser during the adsorption and desorption times, respectively. It is clear to
 332 mention that the rate of enhancement in SDIP is decreased by increasing the switching time due to the decrease
 333 in cycle's number per day. Fig. 5 also shows that there were decrease in the amount of water in cups inside the
 334 evaporator up to 39%, 25% and 0% per one minute by increasing the switching time from one to four minutes,
 335 respectively.

336 Fig. 5(B) shows that the SDWP increased by increasing the switching time to reach a maximum value at 2.5
 337 minutes and then decreased. After this point, the mass production of water in condenser per batch reached

338 steady state while the SDWP dropped down by increasing the switching time. This can be attributed to the
 339 disproportion between the water production and run time per day.

340 Fig. 5(C) shows that by increasing the switching time of the system from one to four minutes, the rate of
 341 enhancement in the COP per one minute is up to 15.4%, 24% and 8%, respectively. This is due to the longer
 342 pre-cooling and pre-heating processes which leads to prepare the adsorber to enhance the adsorption and
 343 desorption processes, respectively, in turn, a large amount of refrigerant vapour will be evaporated and desorbed
 344 from evaporator and bed respectively.

345 As shown in Fig. 5(D), the SDSP is slightly decreased with maximum rate of 6.3% by increasing one minute of
 346 switching time. Despite this decrease in SDSP, there was a small increase in the mass of ice slurry per one
 347 minute up to 1.7%, 6.6% and 0.3% with range of switching time from one to four minute, respectively. This
 348 conflict is caused by disproportion between the increases in run time per day against the mass in of slurry ice in
 349 the evaporator.



355 **Fig. 5.** Effect of switching time on the each of (A) SDIP, mass of solid ice and fresh water in
 356 evaporator, (B) SDSP and mass of ice slurry in evaporator, (C) COP of cooling and (D) SDSP and
 357 mass of ice slurry in the evaporator.
 358
 359
 360
 361

362

363 **6.4 Effect of adsorption/desorption time**

364 Fig. 6 shows the effect of adsorption and desorption time (ADT) on the SDIP, SDSP, SDWP and COP based on
365 the selected switching time of 3 second as stated above. In can be seen from Fig. 6(A) that the SDIP was
366 increased significantly up to 14.7% by increasing the ADT from nine until 11 minutes; however, there were a
367 drop in the SDIP of 2%, 4.9% and 3.4% per two minutes during the ADT from 11 to 17 minutes, respectively.
368 Despite this drop in SDIP, the mass of solid ice increased by up to 25 %, 9.7%, 5.7% and 0.8% per two minutes
369 by increasing of the ADT from nine to 11 minutes, respectively. The main reason of this increase is due to
370 longer time of adsorption and desorption which leads to absorb and release more amount of refrigerant vapour,
371 respectively. Accordingly, the formed ice increased by increasing the ADT. It is worth to mention that there was
372 no water in the cups at ADT of 15 and 17 minutes.

373 Fig. 6(B) shows that the SDWP increased by up to 35% by increasing in the ADT from nine to 11 minutes this
374 can be attributed to the higher amount of desorbed vapour from bed to condenser at the ADT of 11 minutes. The
375 SDWP was continued to increase but with fewer rates until the ADT of 15 min. After the latter ADT, SDWP
376 was dropped by 6% by increasing the ADT to 17 min. This is because the adsorption and desorption processes
377 will be weaker at certain ADT based on the characterization of adsorbent material.

378 Fig. 6(C) shows a significant increase in the COP of the system based on cooling effect up to 10% per two
379 minutes for the ADT from nine to 15 minutes, respectively. This is attributed to that by increasing the ADT
380 from nine to 15 minutes would increase in average drops of antifreeze temperatures up to 2.25, 2.6, 2.7 and 2.85
381 K per two minutes, respectively. After the 15 min, the COP was slightly dropped to 3.4 % due to decrease in the
382 average drop of antifreeze temperature from 2.85 to 2.2 K.

383 Fig. 6(D) shows that the mass of ice slurry was sharply increased up to 22 % by increasing the ADT from nine
384 to 11 minutes. In contrast, the SDSP was decreased by 9.6% at the same period. This is because more heat is
385 absorbed by the antifreeze at longer ADT, in turn; the evaporation process will be increased which leads to
386 produce more ice slurry per batch. But the increase in the ADT has an inversely proportional on the SDSP as the
387 longer ADT leads to decrease the runs number per one day. After the 11 minutes of ADT, the SDSP and mass of
388 slurry ice are fluctuated according to the capacity of adsorbent to absorb the refrigerant vapour will be reduced
389 after certain time. Therefore, the adsorbent material keeps absorbing/desorbing the refrigerant vapour but with
390 insignificant effect.

391

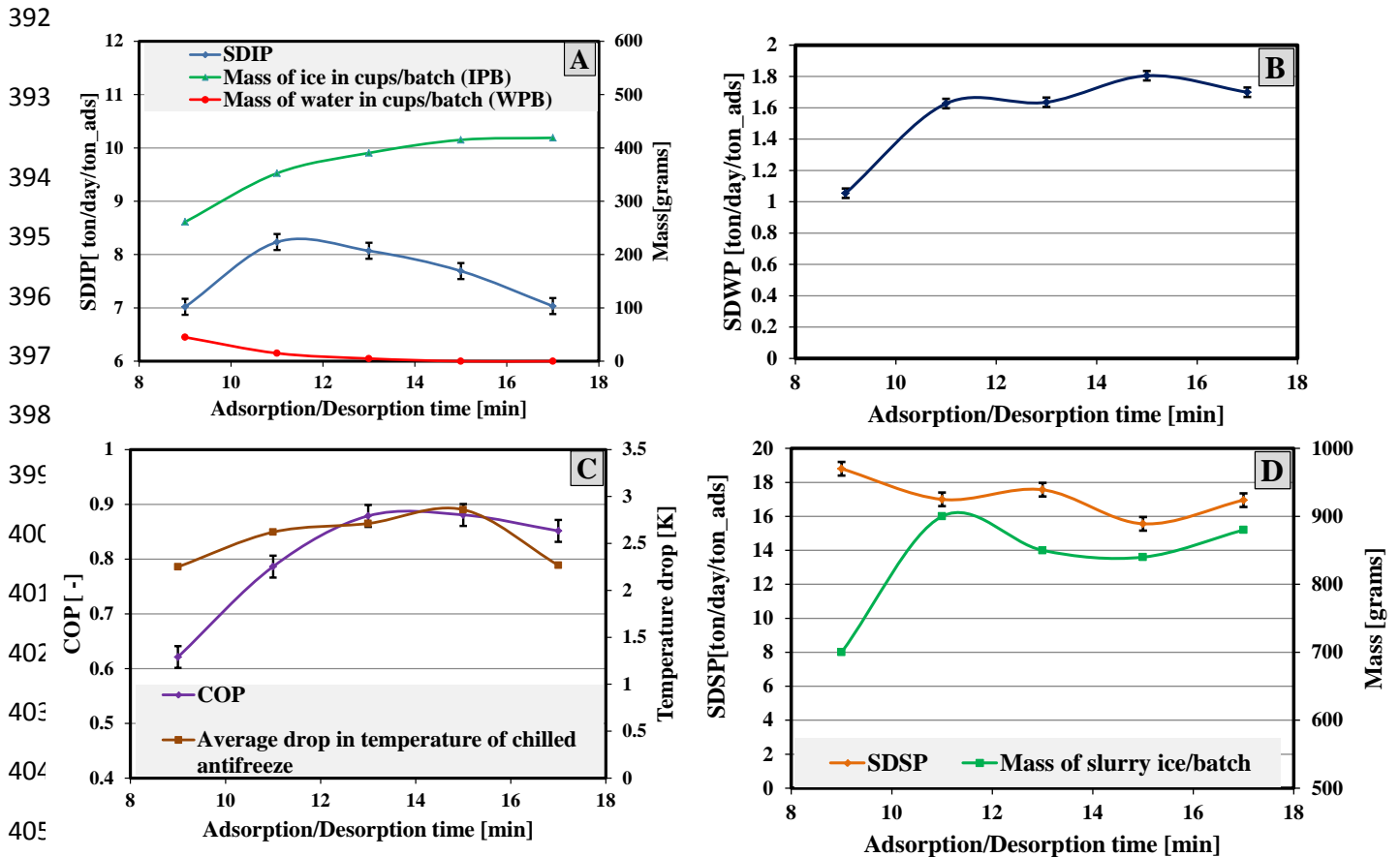


Fig. 6. Effect of adsorption/desorption time on the each of (A) SDIP, mass of solid ice and fresh water in the evaporator, (B) SDWP in the evaporator, (C) COP of cooling and temperature drop in the evaporator, and (D) SDSPP and mass of ice slurry in the evaporator.

7. CONCLUSION

In this work, an advanced technique for adsorption ice making integrated with vacuum direct freeze desalination is developed. The effect of numbers of cycle, switching time, adsorption-desorption time and salinity on the performance of single bed adsorption based on ice making, cooling, ice slurry and desalination using CPO-27 (Ni) MOF-water as working pair was experimentally investigated. Results showed that:

- CPO-27 (Ni) MOF-water working pair shows the potential to be used for ice making application.
- The fresh and sea water can be used as refrigerant in adsorption systems to achieve low evaporation temperature $<0^{\circ}\text{C}$ thus reducing dependence on CFCs and HFCs refrigerants for ice making applications.
- Based on ice production of current system, the optimum number of cycles is three cycles per batch.
- The optimum switching time and adsorption/desorption time are 3 and 15 minutes respectively for producing all outputs.

- 420 • There is an enhancement in SDIP up to 5.4 times with a maximum value up to 8.9 ton/day/ton_ads using
 421 fresh and sea water as refrigerants compared to the maximum value reported in the literature using adsorption
 422 technique with ammonia as refrigerant [5].
- 423 • With this technique, the optimum salinity is 35000 ppm for maximum production of ice up to 8.3
 424 ton/day/ton_ads, COP cooling up to 0.9 and water desalination up to 1.8 ton/day/ton_ads.

425

426 Acknowledgements

427 The authors would like to thank The Higher Committee for Education Development in Iraq (HCED) for
 428 sponsoring the project.

429 References

- 430 [1] R. Critoph, "Towards a one tonne per day solar ice maker," *Renewable Energy*, vol. 9, no. 1,
 431 pp. 626-631, 1996.
- 432 [2] S. M. Ali, and A. Chakraborty, "Adsorption assisted double stage cooling and desalination
 433 employing silica gel+water and AQSOA-ZO2+water systems," *Energy Conversion and*
 434 *Management*, vol. 117, pp. 193-205, 2016.
- 435 [3] H. J. Dakkama, P. Youssef, R. K. Al-Dadah, S. M. Mahmoud, and A.-S. W. A.M, "Adsorption ice
 436 making and freeze water desalination using metal organic framework materials," *Proceeding*
 437 *of ICSAE, IEEE Xplore digital library*, 2016.
- 438 [4] H. J. Dakkama, A. Elsayed, R. K. Al-Dadah, S. M. Mahmoud, and P. Youssef, "Integrated
 439 evaporator–condenser cascaded adsorption system for low temperature cooling using
 440 different working pairs," *Applied Energy*, 2016.
- 441 [5] C. Li, R. Z. Wang, L. W. Wang, T. X. Li, and Y. Chen, "Experimental study on an adsorption
 442 icemaker driven by parabolic trough solar collector," *Renewable Energy*, vol. 57, pp. 223-
 443 233, 2013.
- 444 [6] A. M. Elsayed, H. J. Dakkama, S. Mahmoud, R. Al-Dadah, and W. Kaiyaly, "Sustainable Cooling
 445 Research Using Activated Carbon Adsorbents and Their Environmental Impact," *Applied*
 446 *Environmental Materials Science for Sustainability*, pp. 186-221: IGI Global, 2017.
- 447 [7] R. Wang, L. Wang, and J. Wu, *Adsorption refrigeration technology: theory and application*:
 448 John Wiley & Sons, 2014.
- 449 [8] M. Li, R. Wang, Y. Xu, J. Wu, and A. Dieng, "Experimental study on dynamic performance
 450 analysis of a flat-plate solar solid-adsorption refrigeration for ice maker," *Renewable energy*,
 451 vol. 27, no. 2, pp. 211-221, 2002.
- 452 [9] N. A. A. Qasem, and M. A. I. El-Shaarawi, "Improving ice productivity and performance for an
 453 activated carbon/methanol solar adsorption ice-maker," *Solar Energy*, vol. 98, pp. 523-542,
 454 2013.
- 455 [10] A. P. F. Leite, and M. Dagueuet, "Performance of a new solid adsorption ice maker with solar
 456 energy regeneration," *Energy Conversion and Management*, vol. 41, no. 15, pp. 1625-1647,
 457 2000.
- 458 [11] Z. Li, and K. Sumathy, "A solar-powered ice-maker with the solid adsorption pair of activated
 459 carbon and methanol," *International Journal of Energy Research*, vol. 23, no. 6, pp. 517-527,
 460 1999.

- 461 [12] R. Wang, M. Li, Y. Xu, and J. Wu, "An energy efficient hybrid system of solar powered water
462 heater and adsorption ice maker," *Solar energy*, vol. 68, no. 2, pp. 189-195, 2000.
- 463 [13] D. C. Wang, and J. Y. Wu, "Influence of intermittent heat source on adsorption ice maker
464 using waste heat," *Energy Conversion and Management*, vol. 46, no. 6, pp. 985-998, 2005.
- 465 [14] E. Anyanwu, "Review of solid adsorption solar refrigerator I: an overview of the refrigeration
466 cycle," *Energy conversion and Management*, vol. 44, no. 2, pp. 301-312, 2003.
- 467 [15] H. Z. Hassan, A. A. Mohamad, and H. A. Al-Ansary, "Development of a continuously
468 operating solar-driven adsorption cooling system: Thermodynamic analysis and parametric
469 study," *Applied Thermal Engineering*, vol. 48, pp. 332-341, 2012.
- 470 [16] A. Boubakri, J. Guillemot, and F. Meunier, "Adsorptive solar powered ice maker:
471 experiments and model," *Solar Energy*, vol. 69, no. 3, pp. 249-263, 2000.
- 472 [17] G. Maggio, L. G. Gordeeva, A. Freni, Y. I. Aristov, G. Santori, F. Polonara, and G. Restuccia,
473 "Simulation of a solid sorption ice-maker based on the novel composite sorbent "lithium
474 chloride in silica gel pores"," *Applied Thermal Engineering*, vol. 29, no. 8-9, pp. 1714-1720,
475 2009.
- 476 [18] R. Critoph, "Laboratory testing of an ammonia carbon solar refrigerator."
- 477 [19] Z. Qi, "Study on hybrid system of solar powered water heater and adsorption ice maker,"
478 *International journal of architectural science*, vol. 6, no. 4, pp. 168-172, 2005.
- 479 [20] M. Li, C. J. Sun, R. Z. Wang, and W. D. Cai, "Development of no valve solar ice maker,"
480 *Applied Thermal Engineering*, vol. 24, no. 5-6, pp. 865-872, 2004.
- 481 [21] M. Li, R. Wang, H. Luo, L. Wang, and H. Huang, "Experiments of a solar flat plate hybrid
482 system with heating and cooling," *Applied thermal engineering*, vol. 22, no. 13, pp. 1445-
483 1454, 2002.
- 484 [22] X. Ji, M. Li, J. Fan, P. Zhang, B. Luo, and L. Wang, "Structure optimization and performance
485 experiments of a solar-powered finned-tube adsorption refrigeration system," *Applied
486 Energy*, vol. 113, pp. 1293-1300, 2014.
- 487 [23] S. Kreussler, and D. Bolz, "Experiments on solar adsorption refrigeration using zeolite and
488 water," *Laboratory for Solar Energy, University of Applied Sciences Lubeck*, 2000.
- 489 [24] T. TCHERNEV, "Solar air conditioning and refrigeration systems utilizing zeolites." pp. 209-
490 215.
- 491 [25] Z. S. Lu, R. Z. Wang, L. W. Wang, and C. J. Chen, "Performance analysis of an adsorption
492 refrigerator using activated carbon in a compound adsorbent," *Carbon*, vol. 44, no. 4, pp.
493 747-752, 2006.
- 494 [26] M. Ramos, R. L. Espinoza, M. J. Horn, and A. P. F. Leite, "Evaluation of a zeolite-water solar
495 adsorption refrigerator." pp. 14-19.
- 496 [27] J. Lewis, I. Chaer, and S. Tassou, "Fostering the development of technologies and practices to
497 reduce the energy inputs into the refrigeration of food-Reviews of alternative refrigeration
498 technologies," *Centre for energy and built environment Research school of engineering and
499 design brunel university*, 2007.
- 500 [28] B. Shi, R. Al-Dadah, S. Mahmoud, A. Elsayed, and E. Elsayed, "CPO-27(Ni) metal-organic
501 framework based adsorption system for automotive air conditioning," *Applied Thermal
502 Engineering*, vol. 106, pp. 325-333, 2016.
- 503 [29] P. G. Youssef, H. Dakkama, S. M. Mahmoud, and R. K. Al-Dadah, "Experimental investigation
504 of adsorption water desalination/cooling system using CPO-27Ni MOF," *Desalination*, vol.
505 404, pp. 192-199, 2017.
- 506 [30] E. Elsayed, R. Al-Dadah, S. Mahmoud, P. A. Anderson, A. Elsayed, and P. G. Youssef, "CPO-
507 27(Ni), aluminium fumarate and MIL-101(Cr) MOF materials for adsorption water
508 desalination," *Desalination*, 2016.
- 509 [31] A. Subramani, and J. G. Jacangelo, "Emerging desalination technologies for water treatment:
510 a critical review," *Water Res*, vol. 75, pp. 164-87, May 15, 2015.

511 [32] K. C. Kang, P. Linga, K.-n. Park, S.-J. Choi, and J. D. Lee, "Seawater desalination by gas hydrate
512 process and removal characteristics of dissolved ions (Na⁺, K⁺, Mg²⁺, Ca²⁺, B³⁺, Cl⁻,
513 SO₄²⁻)," *Desalination*, vol. 353, pp. 84-90, 2014.

514 [33] P. Byrne, L. Fournaison, A. Delahaye, Y. Ait Oumeziane, L. Serres, P. Loulergue, A. Szymczyk,
515 D. Mugnier, J.-L. Malaval, R. Bourdais, H. Gueguen, O. Sow, J. Orfi, and T. Mare, "A review on
516 the coupling of cooling, desalination and solar photovoltaic systems," *Renewable and*
517 *Sustainable Energy Reviews*, vol. 47, pp. 703-717, 2015.

518 [34] K. C. Ng, K. Thu, Y. Kim, A. Chakraborty, and G. Amy, "Adsorption desalination: An emerging
519 low-cost thermal desalination method," *Desalination*, vol. 308, pp. 161-179, 2013.

520